Proceedings of the 2000 IEEE
International Conference on Robotics & Automation
San Francisco, CA • April 2000

A Sufficient Condition for Manipulation of Envelope Family

Makoto Kaneko, Kensuke Harada, and Toshio Tsuji

Industrial and Systems Engineering
Hiroshima University
Higashi-Hiroshima 739-8527 JAPAN

Abstract

This paper discusses a sufficient condition for manipulation of Envelope Family, where multiple contacts are allowed between object and chains (or environment). All chains are assigned by either position controlled chain (P-chain) or torque controlled chain (T-chain). While the object motion under multiple contacts can not be uniquely specified by T-chains only, we show a sufficient condition ensuring that a given set of torque commands for T-chains always move the object toward the goal along the surface of P-chain (or a fixed environment). Experiments as well as simulations are also shown to verify the basic idea.

Key words: *Enveloping Grasp, Envelope Family, Manipulation of Object, Envelope Walk.*

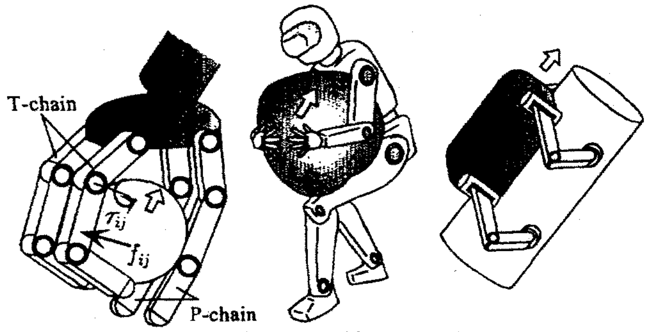

Figure 1: Examples of Envelope Family

1 Introduction

Fig.1 shows a couple of examples of *Envelope Family* where Fig.1(a), (b), and (c) are envelope grasp by a robot hand, manipulation of a huge and heavy object by a humanoid robot, and envelope walk by a legged robot, respectively. Each robot in *Envelope Family* has a common working style where multiple contacts are allowed between chains and object (or environment). For a manipulation of object or body, so far, many researchers have focused on the link tip level manipulation or locomotion, since a dexterous motion can be anticipated by utilizing many degrees of freedom existing in the system. Such manipulation or locomotion, however, may easily fail in grasping an object under an external disturbance or in standing over the ground with a steep slope. On the other hand, due to multiple contacts, manipulation or locomotion in enveloping style can be expected even more robustness than that in tip level one. Also, this type of manipulation or locomotion greatly contributes to suppressing the peak torque by distributing the gravitational force to each contact point. In a humanoid robot as shown in Fig.1(b), the manipulation in enveloping style may provide the only feasible solution under joint torque limitation.

While we can find such advantages for the manipulation in enveloping style, there are a couple of barriers to break through for achieving it. The biggest one is that the total force produced by all contact forces is not uniquely determined, due to the one-to-multiple mapping from the joint torque to the contact force. As a result, the moving direction of object is not uniquely specified either. To make us release from the mapping problem, we give up manipulating an enveloped object by pure torque control. Instead, we assign all chains (fingers or legs) into position controlled chain (P-chain) and torque controlled chain (T-chain), respectively, where P-chain might be replaced by an environment. Now, let us consider a sphere enveloped by a robot hand as shown in Fig.1(a), where four fingers are categorized into T-chains and P-chains. T-chains and P-chains can be regarded as pushers and supports, respectively. The object will move along the surface of P-chains, if we impart an appropriate set of torque commands for the T-chains. Under such multiple contacts, a rolling motion may occur at a particular contact point, while sliding motions happen at most contact points. We do not care what kinds of motion actually happen during the manipulation process. The goal of this paper is to obtain a sufficient condition ensuring that a given set of torque for T-chains always move the object toward the designated direction along the surface of P-chains (or environment).

Assuming that each contact force set is bounded and each link has one contact point with an object, we begin by showing that the contact force set is always bounded within the friction cone intersected by two parallel planes (Theorem 1). Approximating each friction cone by a convex polyhedral cone, we show that a vertex of total force set always corresponds to a contact force lying on one of span vectors on the approximated friction cone, while the opposite flow is not always true (Theorem 2 and Theorem 3). We also show that if a convex polyhedral cone includes the original friction cone, the total force set under the polyhedral cone always includes the one under the original friction cone (Theorem 4). Based on these properties, we introduce a sufficient condition for putting the total force set under the original friction cone into the bounded space (Theorem 5), where the object always receives an enough force to break the contact over the surface of P-chains. To verify our basic idea, we show some experiments as well as simulations. While we complete our formulation for an enveloping grasp by a multifingered robot hand, the result is available for the whole Envelope Family.

2 Related Work

Salisbury [1] has proposed the basic concept of whole-arm manipulation by taking various advantages, such as the potential capability of a large payload and the robustness of holding an object against an external disturbance. Trinkle, Abel, and Paul [2] have discussed the grasp planning issue for enveloping a planar frictionless object. As far as we know, "Enveloping Grasp" as a terminology has first appeared in the paper. For an external disturbance, some enveloping grasps can automatically generate a counter force (or moment) to some extent without changing the joint torque. Enveloping grasp having this characteristics is particularly termed "Power Grasp" [3]-[8]. Mirza and Orin [3] have pointed out that power grasps maximize the load capability and are highly stable in nature because of a large number of distributed contact points on the grasped object. They applied a linear programming approach to formulate and solve the force distribution problem in power grasps and showed a significant increase in the maximum weight. Bicchi [4] has addressed the problem of force decomposition in power grasps and showed that internal forces allowing inner link contacts can be decomposed into active and passive ones. Zhang, Nakamura, Goda, and Yoshimoto [5] have provided the measure of the robustness of power grasp, where they evaluate the robustness by the minimum virtual work which breaks a contact between the finger link and the object. Zhang and Gruver [6] have defined the power grasp mathematically and analyzed the force distribution at the contact points. Omata and Nagata [7] have shown the possible area of contact forces by utilizing the constraint condition obtained by the kinematic relationship. Yu, Takeuchi, and Yoshikawa [8] have proposed a procedure for achieving the power grasp optimization, where they searched the optimal configuration providing the minimum joint torque set for a given admissible external force space. These works [3]-[8] discussed how firmly the hand can grasp the object. On the other hand, we relax the grasping force and address the manipulation issue for an enveloped object. In our former work [9], we discussed how the enveloped object behaves under a given set of torque and proposed the Force-Flow Diagram for judging whether a global motion of the object appears or not. It can be regarded that the work [9] deals with a direct problem, where we examine the motion behavior for a given set of torque. On the other hand, this paper discusses, in some sense, an inverse problem, namely, we pursue the torque command enabling the object to always push the position controlled finger and to break the frictional limit at contact points with P-chains.

3 A Sufficient Condition for Manipulation

3.1 Main Assumption

To simplify the discussion, we set the following assumptions.

Assumption 1: The robot hand has n T-chains and m rotational joints per chain. Every joint axis in the i-th chain is parallely arranged.

Assumption 2: Each link in T-chains has one contact with the object.

Assumption 3: Mass of link is negligible.

Assumption 4: At each contact point, we assume a Coulomb friction whose coefficient is given by μ, where both static and dynamic frictional coefficients are not distinguished.

Assumption 5: Positions of contact points and the center of gravity of the object are both measurable.

Assumption 6: Each joint has a joint position sensor and a joint torque sensor.

Assumption 7: Interference among chains is ignored.

Assumption 8: Each joint actuator has its torque limitation τ^{max}.

Assumption 9: Small compliance is assumed at each contact point, while the deformation due to the compliance is neglected.

For a rigid body system with multiple contact points, an indeterminate contact force often appears at each contact point[4], [6], [7], [10]. With Assumption 9, we are perfectly released from the issue caused by the indeterminate contact force, and the total force set by summing up all contact forces keeps convex. For a further analysis, however, we do not utilize any compliance matrix explicitly at each contact point. Instead, we consider all possible contact forces within the friction cone for a given set of torque, which is equivalent to considering various compliance matrices at each contact point.

3.2 Mapping from Torque to Contact Force

Let us consider the i-th T-chain of a robot hand as shown in Fig.1(a), where $\boldsymbol{f}_{ij}$ and $\boldsymbol{\tau}_i = [\tau_{i1}, \cdots, \tau_{im}]^t \in R^{m\times 1}$ denote the contact force vector at the j-th contact point of the i-th chain, and the joint torque vector of the i-th chain, respectively. We have the following relationship $\boldsymbol{\tau}_i^j = \boldsymbol{J}_{ij}^t \boldsymbol{f}_{ij}$ between $\boldsymbol{\tau}_i^j$ and $\boldsymbol{f}_{ij}$, where $\boldsymbol{J}_{ij}^t$ denotes the transpose of Jacobian matrix mapping the contact force into the joint torque. By utilizing the principle of superposition for the relationship between $\boldsymbol{\tau}_i^j$ and $\boldsymbol{f}_{ij}$, $\boldsymbol{\tau}_i$ is given by $\boldsymbol{\tau}_i = \sum_{j=1}^{m} \boldsymbol{J}_{ij}^t \boldsymbol{f}_{ij}$. Therefore, the relationship between the contact force and the joint torque for the i-th T-chain is expressed by,

$$\boldsymbol{\tau}_i = \boldsymbol{J}_i^t \boldsymbol{f}_i \tag{1}$$

where $\boldsymbol{f}_i = [\boldsymbol{f}_{i1}^t, \cdots, \boldsymbol{f}_{im}^t]^t \in R^{3m\times 1}$, and

$$\boldsymbol{J}_i^t = [\boldsymbol{J}_{i1}^t, \cdots, \boldsymbol{J}_{im}^t] \tag{2}$$

$$= \begin{bmatrix} \boldsymbol{J}_{i11}^t & & \boldsymbol{J}_{i1m}^t \\ & \ddots & \\ \boldsymbol{o} & & \boldsymbol{J}_{imm}^t \end{bmatrix} \in R^{m\times 3m} \tag{3}$$

Hereafter, to avoid the complicated notation, we often neglect the subscript showing the i-th chain as far as it is not necessary.

While both the contact and the total forces span convex sets unless any indeterminate contact force appears. It is interesting to know under what condition the total force becomes maximum (or minimum) in a designated direction. The most likely case may be that it occurs when every contact force lies on the friction boundary. Is it always true? To answer the question, we begin by introducing the following definition and theorem.

[Definition] *It is called contact-force-bounded, if the contact force spans a bounded set within the friction cone. It is called contact-force-open, if the contact force spans an open set within the friction cone.*

It should be noted that under a constant torque control, one link system contacting with an object always results in the contact-force-bounded in 2D but not always in 3D. Hereafter, we assume that the contact-force-bounded is satisfied at each contact point.

[**Theorem 1**] *Suppose a T-chain under constant torque control. Under the contact-force-bounded, each contact force spans a convex set constructed with the friction cone intersected by two parallel planes.*

[**Proof**] Since the Jacobian $\boldsymbol{J}$ is an upper triangular matrix (see eq.(3)), for the mm component, we can find the relationship of $\tau_m = \boldsymbol{J}_{mm}^t \boldsymbol{f}_m$. By solving the equation with respect to $\boldsymbol{f}_m$,

$$\boldsymbol{f}_m = (\boldsymbol{J}_{mm}^t)^\sharp \tau_m + \{\boldsymbol{I}_3 - (\boldsymbol{J}_{mm}^t)^\sharp \boldsymbol{J}_{mm}^t\}\boldsymbol{w}_m \tag{4}$$

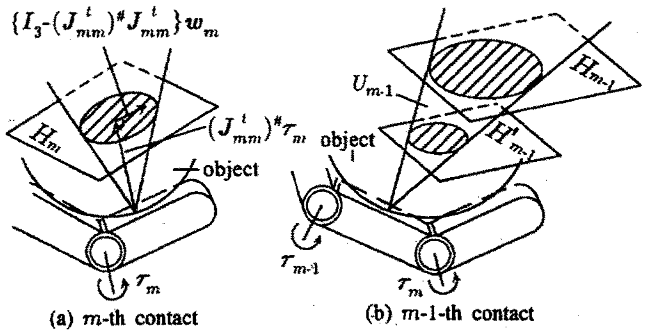

Figure 2: Contact force sets in m and m-1 contacts

where $\boldsymbol{w}_m \in R^{3\times 1}$ and $\sharp$ denote an arbitrary vector and the seudo-inverse matrix, respectively, and $\boldsymbol{f}_m \in R^{3\times 1}$, $\boldsymbol{J}_{mm}^t \in R^{1\times 3}$ and $\boldsymbol{I}_3 \in R^{3\times 3}$ (Identical Matrix), respectively. Since rank$(\boldsymbol{J}_{mm}^t) = 1$, rank$(\boldsymbol{I}_3 - (\boldsymbol{J}_{mm}^t)^\sharp \boldsymbol{J}_{mm}^t) = 2$, which means that there exists only two independent parameters in $\boldsymbol{w}_m$ and, therefore, $\{\boldsymbol{I}_3 - (\boldsymbol{J}_{mm}^t)^\sharp \boldsymbol{J}_{mm}^t\}\boldsymbol{w}_m$ spans a plane. Due to the orthogonal relationship between $(\boldsymbol{J}_{mm}^t)^\sharp \tau_m$ and $\{\boldsymbol{I}_3 - (\boldsymbol{J}_{mm}^t)^\sharp \boldsymbol{J}_{mm}^t\}\boldsymbol{w}_m$, we have the geometrical representation as shown in Fig.2(a), where the hatched area denotes the contact force set under constant torque control. For the last link, the contact force set can be regarded as the cross section of the friction cone intersected by two parallel planes whose distance is zero. Now, let us consider the contact force $\boldsymbol{f}_{m-1}$ by fixing $\boldsymbol{w}_m = \boldsymbol{w}_{m0}$. From the relationship between the torque and the contact force, we obtain,

$$\tau_{m-1} = \boldsymbol{J}_{m-1m-1}^t \boldsymbol{f}_{m-1} + \boldsymbol{J}_{m-1m}^t \boldsymbol{f}_m \tag{5}$$

$$= \boldsymbol{J}_{m-1m-1}^t \boldsymbol{f}_{m-1} + \boldsymbol{J}_{m-1m}^t\{(\boldsymbol{J}_{mm}^t)^\sharp \tau_m + \boldsymbol{B}_m \boldsymbol{w}_{m0}\} \tag{6}$$

where $\boldsymbol{B}_m = \boldsymbol{I}_3 - (\boldsymbol{J}_{mm}^t)^\sharp \boldsymbol{J}_{mm}^t \in R^{3\times 3}$. The second term of the right hand side of eq.(6) is constant, because both τ_m and $\boldsymbol{w}_{m0}$ are constant. Replacing the second term of the right hand side by τ'_{m-1}, eq.(6) is rewritten into the following form.

$$\tau_{m-1} - \tau'_{m-1} = \boldsymbol{J}_{m-1m-1}^t \boldsymbol{f}_{m-1} \tag{7}$$

where $\tau'_{m-1} = \boldsymbol{J}_{m-1m}^t\{(\boldsymbol{J}_{mm}^t)^\sharp \tau_m + \boldsymbol{B}_m \boldsymbol{w}_{m0}\}$. From eq.(7), we can obtain

$$\boldsymbol{f}_{m-1} = (\boldsymbol{J}_{m-1m-1}^t)^\sharp \tau_{m-1}^* + \boldsymbol{B}_{m-1}\boldsymbol{w}_{m-1} \tag{8}$$

where $\tau_{m-1}^* = \tau_{m-1} - \tau'_{m-1}$. By changing the vector $\boldsymbol{w}_m$ in $\boldsymbol{H}_m$, we can obtain the contact force set $\boldsymbol{U}_{m-1}$, as shown in Fig.2(b). Note that two planes $\boldsymbol{H}_{m-1}$ and $\boldsymbol{H}'_{m-1}$ are parallel each other, since the direction of $(\boldsymbol{J}_{m-1m-1}^t)^\sharp \tau_{m-1}^*$ does not change while τ_{m-1}^* varies depending upon $\boldsymbol{w}_m$. Therefore, $\boldsymbol{U}_{m-1}$ is bounded with the m-1-th friction cone intersected by two parallel planes. Now, suppose that the contact force $\boldsymbol{f}_j$ spans a convex set constructed by two parallel planes $\boldsymbol{H}_j$ and $\boldsymbol{H}'_j$ cutting the friction cone. Under this assumption, we consider the contact force f_{j-1}. By the assumption, f_j can be expressed by

$$f_j = (J_{jj}^t)^\sharp\{\tau_{jmin}^* + (\tau_{jmax}^* - \tau_{jmin}^*)\eta_j\} + B_j w_j \quad (9)$$

where η_j is the parameter determining the magnitude in the direction of $(J_{jj}^t)^\sharp$ and $0 \le \eta_j \le 1$. The former discussions prove that f_{j-1} spans a plane under $\eta_j = \eta_{j0}$ and $w_j = w_{j0}$. By changing w_j under $\eta_j = \eta_{j0}$, we can easily show that the contact force set is bounded with the i-1-th friction cone intersected by two parallel planes. These discussions can be further extended that the contact force set U_{j-1} is bounded by two parallel planes cutting the friction cone even when both w_j and η_j are changed, which proves the theorem. □

This theorem guarantees that each friction cone is never cut by more than two planes. This nature of the boundary provides a good hint for determining where each contact force lies, when the total force becomes maximum (or minimum).

3.3 Friction cone approximation

In order to change from nonlinear to linear friction constraint, we approximate the i-th friction cone of the i-th chain by the L faced polyhedral convex cone[11], [12].

$$f_{ij} = \sum_{l=1}^{L} \lambda_{ij}^l v_{ij}^l \quad (\lambda_{ij}^l \ge 0) \quad (10)$$

$$= V_{ij}\lambda_{ij} \quad (11)$$

where $V_{ij} = [v_{ij}^1, \cdots, v_{ij}^L] \in R^{3\times L}$ and $\lambda_{ij} = [\lambda_{ij}^1, \cdots, \lambda_{ij}^L]^t \in R^{L\times 1}$. For the i-th chain, we obtain the following form.

$$f_i = V_i\lambda_i \quad (12)$$

where $\lambda_i = [\lambda_{i1}^t, \cdots, \lambda_{im}^t]^t \in R^{Lm\times 1}$, and

$$V_i = \begin{bmatrix} V_{i1} & & o \\ & \ddots & \\ o & & V_{im} \end{bmatrix} \in R^{3m\times Lm} \quad (13)$$

From eq.(1) and (12),

$$\tau_i = J_i^t V_i \lambda_i \quad (14)$$

For n fingers, we obtain

$$\begin{bmatrix} \tau_1 \\ \vdots \\ \tau_n \end{bmatrix} = \begin{bmatrix} J_1^t V_1 & & o \\ & \ddots & \\ o & & J_n^t V_n \end{bmatrix} \begin{bmatrix} \lambda_1 \\ \vdots \\ \lambda_n \end{bmatrix}. \quad (15)$$

By solving eq.(15) with resppect to $\lambda = [\lambda_1^t \cdots \lambda_n^t]^t \in R^{Lmn\times 1}$,

$$\lambda = H^\sharp \tau + (I_{Lmn} - H^\sharp H)x \quad (16)$$

where

$$H = \begin{bmatrix} J_1^t V_1 & & o \\ & \ddots & \\ o & & J_n^t V_n \end{bmatrix},$$

$x \in R^{Lmn\times 1}$ denotes an arbitrary vector, and $\sharp$ shows the pseudo-inverse. Since $\lambda \in R^{Lmn\times 1}$ and $\tau = [\tau_1, \cdots, \tau_n]^t \in R^{mn\times 1}$, x has $(L-1)nm$ independent parameters under a full rank matrix H. Thus eq.(16) can be rewritten as follows:

$$\lambda = H^\sharp \tau + N\Phi, \quad (17)$$

where $\Phi \in R^{(L-1)mn\times 1}$ is an arbitrary vector and $N \in R^{Lmn\times(L-1)mn}$ is the full rank matrix satisfying H $N = o$. As a result, the total force of the center of gravity of object f_o is expressed by

$$f_o = EV\{H^\sharp \tau + N\phi\} \quad (18)$$

where

$$E = [I_3, \cdots, I_3] \in R^{3\times 3mn}$$

$$V = \begin{bmatrix} V_1 & & o \\ & \ddots & \\ o & & V_n \end{bmatrix}.$$

3.4 Relationship between total force and contact force sets

We now come back to the question where each contact force lies when the total force becomes maximum (or minimum) in the designated direction. To answer the question, we introduce two theorems, Theorem 2 reviews general properties on a polyhedral convex set and Theorem 3 describes the inherent relationship between contact force and total force sets.

[Theorem 2] *Let $C_i (i = 1, \cdots, n)$ be a polyhedral convex set. Define $C = C_1 + \cdots + C_n$, where $C_1 + \cdots + C_n \triangleq \{x_1 + \cdots + x_n \mid x_i \in C_i (i = 1, \cdots, n)\}$. (1) C is a polyhedral convex set. (2) Each vertex in C always corresponds to a vertex in C_i, while a vertex in C_i does not always correspond to a vertex in C.*

[Proof] See appendix.

[Theorem 3] *For the i-th T-chain with m contacts, suppose that each friction cone is modeled by a convex polyhedral cone and contact-force-bounded is guaranteed. Under constant torque control, each $f_{ij} (j = 1, \cdots, m)$ always lies on one of span vectors v_{ij}^l of the cone, when f_{oi} becomes maximum (or minimum) in a certain direction.*

[Proof] From Theorem 1, each contact force $f_{ij} (j = 1, \cdots, m)$ spans a convex polyhedral set constructed by two parallel planes cutting the approximated convex polyhedral cone. Let C_{ij} be the j-th convex polyhedral set of the i-th chain. Since every vertex in C_{ij} appears only

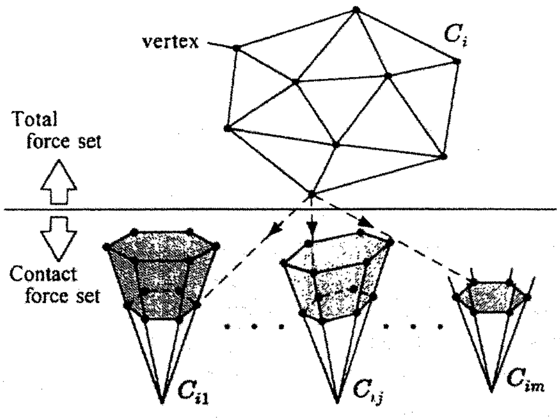

Figure 3: Corresponding relationship between vertex

on span vectors under contact-force-bounded as shown in Fig.3, Theorem 2 guarantees that a vertex in the convex polyhedral set spanned by $\boldsymbol{f}_{oi}$ always corresponds to a contact force lying on one of span vectors, as shown in Fig.3, which holds the theorem. □

Theorem 3 allows us to focus on the contact force coinciding with a span vector, when discussing the boundary of total force set. From Theorem 3, we can set $\lambda_{ij}^{k_j} \geq 0 (k = k_j)$ and $\lambda_{ij}^{k} = 0 (k \neq k_j)$ for $\lambda_{ij}^{k} (k = 1, \cdots, L)$, such that we can find the boundary of the total force set for the i-th T-chain. Based on this property, we introduce the following two constraints.

$$\boldsymbol{S}\boldsymbol{\lambda} \geq \mathbf{o} \tag{19}$$
$$\boldsymbol{S}^*\boldsymbol{\lambda} = \mathbf{o} \tag{20}$$

where

$$\boldsymbol{S} = \begin{bmatrix} \boldsymbol{S}_1 & & \mathbf{o} \\ & \ddots & \\ \mathbf{o} & & \boldsymbol{S}_n \end{bmatrix}, \boldsymbol{S}^* = \begin{bmatrix} \boldsymbol{S}_1^* & & \mathbf{o} \\ & \ddots & \\ \mathbf{o} & & \boldsymbol{S}_n^* \end{bmatrix}$$

$$\boldsymbol{S}_i = \begin{bmatrix} \boldsymbol{e}_{k1}^t & & \mathbf{o} \\ & \ddots & \\ \mathbf{o} & & \boldsymbol{e}_{km}^t \end{bmatrix} \in R^{m \times Lm} \tag{21}$$

$$\boldsymbol{S}_i^* = \begin{bmatrix} \boldsymbol{\Gamma}_1 & & \mathbf{o} \\ & \ddots & \\ \mathbf{o} & & \boldsymbol{\Gamma}_m \end{bmatrix} \in R^{(L-1)m \times Lm} \tag{22}$$

$$\boldsymbol{\Gamma}_j = [\boldsymbol{e}_1, \cdots, \boldsymbol{e}_{kj-1}, \boldsymbol{e}_{kj+1}, \cdots, \boldsymbol{e}_L]^t \in R^{(L-1) \times L} \tag{23}$$

$$\boldsymbol{e}_{kj} = [\underbrace{0, \cdots, 0,}_{1,\cdots,k_j-1,} \underbrace{1,}_{k_j,} \underbrace{0, \cdots, 0}_{k_j+1,\cdots,L}]^t \in R^{L \times 1} \tag{24}$$

Eq.(20) is for keeping each contact force in the pushing direction for the object, and eq.(21) is for making each contact force adhere to one ridge. Since $\boldsymbol{S}^* \in R^{(L-1)mn \times Lmn}$ and $\boldsymbol{N} \in R^{Lmn \times (L-1)mn}$ are full rank, $\boldsymbol{S}^*\boldsymbol{N}$ becomes a nonsingular matrix. From eq.(17) and eq.(21), $\boldsymbol{\Phi}$ is obtained as follows:

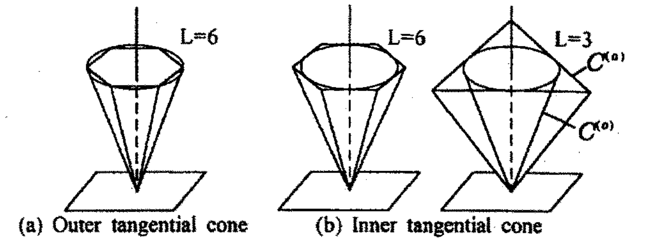

Figure 4: Several polyhedral convex cones

$$\boldsymbol{\Phi} = -\boldsymbol{D}^{-1}\boldsymbol{S}^*\boldsymbol{H}^\sharp\boldsymbol{\tau}, \tag{25}$$

where

$$\boldsymbol{D} = \boldsymbol{S}^*\boldsymbol{N}. \tag{26}$$

Substituting $\boldsymbol{\Phi}$ into eq.(17) and ineq.(20), we obtain

$$\boldsymbol{S}\left(\boldsymbol{I} - \boldsymbol{N}\boldsymbol{D}^{-1}\boldsymbol{S}^*\right)\boldsymbol{H}^\sharp\boldsymbol{\tau} \geq \mathbf{o}. \tag{27}$$

Also, by utilizing eq.(26), the total force set can be expressed in the following form.

$$\boldsymbol{f}_o = \boldsymbol{E}\boldsymbol{V}\left(\boldsymbol{I} - \boldsymbol{N}\boldsymbol{D}^{-1}\boldsymbol{S}^*\right)\boldsymbol{H}^\sharp\boldsymbol{\tau} \tag{28}$$

By changing k_j, we finally obtain L^{mn} set of inequalities and equations given by ineq.(28) and eq.(29), respectively. We note that eq.(29) includes joint torque $\boldsymbol{\tau}_i$ explicitly. By utilizing eq.(29), we can discuss how to determine the command torque, so that the object may move in a bounded direction along P-chains (or environment). Now, recall that each friction cone is approximated by a polyhedral convex cone. By this approximation, we can no more keep the exactness for both the contact and the total force sets. This causes that either the total force set may be produced by the contact force never existing actually, or it dose not include the contact force existing under the actual friction cone. To make clear the relationship between two total force sets obtained under the approximated friction cone and under the actual one, we introduce the following theorem.

[Theorem 4] *Suppose a T-chain under constant torque control and contact-force-bounded. Let $C^{(1)}$ and $C^{(2)}$ ($C^{(1)} \subseteq C^{(2)}$) be two polyhedral convex cones. Also, let $\mathcal{F}^{(1)}$ and $\mathcal{F}^{(2)}$ be contact force sets produced under $C^{(1)}$ and $C^{(2)}$, respectively. When $\mathcal{V}^{(i)} = \mathcal{F}_1^{(i)} + \mathcal{F}_2^{(i)} + \cdots + \mathcal{F}_m^{(i)} (i = 1 or 2)$, $\mathcal{V}^{(1)} \subseteq \mathcal{V}^{(2)}$ is always guaranteed, where $\mathcal{F}_1^{(i)} + \cdots + \mathcal{F}_m^{(i)} \triangleq \{\boldsymbol{x}_1^{(i)} + \cdots + \boldsymbol{x}_m^{(i)} \mid \boldsymbol{x}_j^{(i)} \in \mathcal{F}_j^{(i)} (j = 1, \cdots, m)\}$.*

[Proof] For the m-th link, since the plane produced by $\boldsymbol{B}_m\boldsymbol{w}_m$ expresses the cross section of the m-th friction cone, $\mathcal{F}_m^{(1)} \subseteq \mathcal{F}_m^{(2)}$ is obvious. Now, suppose $\mathcal{F}_k^{(1)} \subseteq$

$\mathcal{F}^{(2)}_k (k = i, \cdots, m)$. Under this assumption, we consider the contact force $\boldsymbol{f}_{i-1}$. From eq.(3), we have

$$\boldsymbol{f}_{i-1}=(\boldsymbol{J}^t_{i-1i-1})^{\sharp}(\tau_{i-1}-\sum_{k=i}^{m}\boldsymbol{J}^t_{j-1k}\boldsymbol{f}_k)+\boldsymbol{B}_{i-1}\boldsymbol{w}_{i-1} \quad (29)$$

By assumption, $\mathcal{F}^{(1)}_k \subseteq \mathcal{F}^{(2)}_k$ exists for $\boldsymbol{f}_k (k = i, \cdots, m)$, and the plane produced by $\boldsymbol{B}_{i-1}\boldsymbol{w}_{i-1}$ expresses the cross section of the $i-1$-th friction cone. Since $\boldsymbol{f}_{i-1}$ is expressed by a linear combination of $\boldsymbol{f}_k (k = i, \cdots, m)$ and $\boldsymbol{B}_{i-1}\boldsymbol{w}_{i-1}$, $\mathcal{F}^{(1)}_{i-1} \subseteq \mathcal{F}^{(2)}_{i-1}$ exists. Therefore, by the mathematical induction, $\mathcal{F}^{(1)}_k \subseteq \mathcal{F}^{(2)}_k$ exists for every k. Since $\mathcal{V}^{(i)}$ is expressed by a linear combination of $\mathcal{F}^{(i)}_k (i = 1, 2, k = 1, \cdots, m)$, $\mathcal{V}^{(1)} \subseteq \mathcal{V}^{(2)}$ is ensured. □

For example, let $C^{(o)}$ and $C^{(a)}$ ($C^{(o)} \subseteq C^{(a)}$) be the original and an approximated friction cones, respectively. This relationship is illustrated in Fig.3(b). Also, let $\mathcal{V}^{(o)}$ and $\mathcal{V}^{(a)}$, be the total force sets obtained under $C^{(o)}$ and $C^{(a)}$, respectively. Since $C^{(o)} \subseteq C^{(a)}$, Theorem 4 ensures $\mathcal{V}^{(o)} \subseteq \mathcal{V}^{(a)}$. Now, let $\mathcal{V}^{(d)}$ be a desired total force set where a desired object's motion is expected. If a set of torque commands are chosen so that $\mathcal{V}^{(a)} \subseteq \mathcal{V}^{(d)}$, $\mathcal{V}^{(o)} \subseteq \mathcal{V}^{(d)}$ is always guaranteed. This means that the total force set under the original friction cone also produces a desired motion for the object. This nature is important for keeping a sufficiency of manipulation of an enveloped object.
Now, the remaining questions are as follows:
(1) How to design $\mathcal{V}^{(d)}$?
(2) How to determine a set of torque commands so that $\mathcal{V}^{(a)} \subseteq \mathcal{V}^{(d)}$ may be satisfied ?

3.5 Design of $\mathcal{V}^{(d)}$

For simplifying the discussion, we assume a single T-chain whose contact points exist on the plane parpendicular to the environment and includes the center of gravity of object. We also assume that an object can support moments around both x and z axes in Fig.5, while a rolling motion around y axes is allowed. These assumptions enable us to focus on the object's motion in x-z plane as shown in Fig.5(b). Now, consider the space $\mathcal{V}^{(d)}$ sandwiched by planes Π_1 and Π_2, where Π_1 and Π_2 are parallel to the environment and the right boundary of the friction cone at the point of contact with environment, respectively. Mathematically, $\mathcal{V}^{(d)}$ is given by

$$\mathcal{V}^{(d)} = \mathcal{V}^{(1)} \cap \mathcal{V}^{(2)} \quad (30)$$

$$\mathcal{V}^{(i)} = \{\boldsymbol{p} | \boldsymbol{c}^t_{ai}\boldsymbol{p} \geq 0\} \quad (31)$$

where $\boldsymbol{p}$ expresses an arbitrary point in $\mathcal{V}^{(i)}$ and $\boldsymbol{c}_{ai}$ denotes a unit vector indicating the normal direction of Π_i, as shown in Fig.5(b) and Fig.6(a). $\mathcal{V}^{(1)}$ and $\mathcal{V}^{(2)}$ are for making the object keep contact with the environment and for producing slipping motion at the point of contact

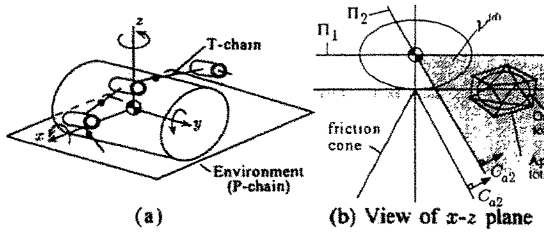

Figure 5: Design of $\mathcal{V}^{(d)}$

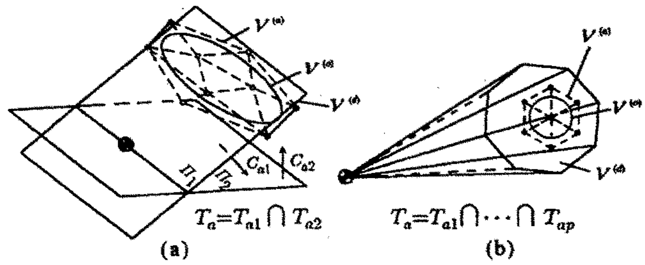

Figure 6: Relationship among $\mathcal{V}^{(o)}$, $\mathcal{V}^{(a)}$, and $\mathcal{V}^{(d)}$

with environment, respectively. If the total force set $\mathcal{V}^{(a)}$ ($\supseteq \mathcal{V}^{(o)}$) is put in $\mathcal{V}^{(d)}$, there exists no total force that can balance with a contact force within the friction cone between the object and environment. This means that the object can not remain stationary and inevitably moves toward -x direction while keeping contact with the environment. Of course, in order to restrict the object's motion we can impart constraints more than two, by adding $\mathcal{V}^{(3)}$, $\mathcal{V}^{(4)}$, $\cdots$, $\mathcal{V}^{(p)}$ as shown in Fig.6(b).

3.6 Determination of command torque set T_c

Let $\boldsymbol{f}_o$ be the total force set produced by all T-chains. The condition for putting all possible $\boldsymbol{f}_o$ into a semi-infinite region $\mathcal{V}^{(i)}$ is given by $\boldsymbol{c}^t_{ai}\boldsymbol{f}_o \geq 0$ or

$$\boldsymbol{c}^t_{ai}\, \boldsymbol{E}\boldsymbol{V}\left(\boldsymbol{I} - \boldsymbol{N}\boldsymbol{D}^{-1}\boldsymbol{S}^*\right)\boldsymbol{H}^{\sharp}\boldsymbol{\tau} \geq 0 \quad (32)$$

By taking all combinations among span vectors, we have totally L^{mn} inequalities for both ineq.(28) and (33).
For n T-chains, ineq.(28) and (33) can be rewritten in the following form, respectively.

$$\boldsymbol{A}_1\boldsymbol{\tau} \geq 0 \quad (33)$$

$$\boldsymbol{A}_{2i}\boldsymbol{\tau} \geq 0 \quad (34)$$

where $\boldsymbol{\tau} = [\boldsymbol{\tau}^t_1, \cdots, \boldsymbol{\tau}^t_n]^t$, and $\boldsymbol{A}_1$ and $\boldsymbol{A}_{2i}$ are coefficient matrices composed of $\boldsymbol{S}\left(\boldsymbol{I} - \boldsymbol{N}\boldsymbol{D}^{-1}\boldsymbol{S}^*\right)\boldsymbol{H}^{\sharp}$ and $\boldsymbol{c}^t_{ai}\boldsymbol{E}\boldsymbol{V}\left(\boldsymbol{I} - \boldsymbol{N}\boldsymbol{D}^{-1}\boldsymbol{S}^*\right)\boldsymbol{H}^{\sharp}$, respectively. The common space in ineq.(34), (35) and torque limitation provides the torque space T_{ai} ensuring the object's motion along P-chain.

$$T_{ai} = \{\boldsymbol{\tau} | \boldsymbol{A}_i\boldsymbol{\tau} \geq 0 \cap \boldsymbol{\tau}^{min} \leq \boldsymbol{\tau} \leq \boldsymbol{\tau}^{max}\} \quad (35)$$

where $A_i = [A_{1i}^t, A_{2i}^t]^t$. T_{ai} provides the basic form when determining the command torque set T_c.

[Theorem 5] *Let $\mathcal{D} = \mathcal{V}^{(1)} \cap \cdots \cap \mathcal{V}^{(p)}$ be a polyhedral convex cone whose top coincides with the center of gravity of the object. A sufficient condition for producing the total force set within $\mathcal{D}$ is given by*

$$T_c \neq \phi \qquad (36)$$

where $T_c = T_{a1} \cap \cdots \cap T_{ap}$
[Proof] Omitted. □

To find a set of command torque, we change torque step by step and examine whether they satisfy the condition (36) or not. We continue this procedure until we can find at least one solution. To efficiently reach a solution, we change torque with a large step from the minimum to the maximum values. If no solution, then the initial value is shifted a bit and the same procedure is repeated. This way is generally effective for reaching a solution in the possible torque space.

3.7 Simulation

Fig.7(a) shows an example of 2D model, where we assume one T-chain and one P-chain. We discuss an issue in which the object is moved from the initial position to the upper direction along the P-chain, where $l = 1[m], R = 0.3[m], mg = 1.0[N]$, $\tau_1^{min} = 0.0[Nm]$, $\tau_1^{max} = 2.5[Nm]$, $\tau_2^{min} = 0.0[Nm]$, $\tau_2^{max} = 1.0[Nm]$ and $\alpha = tan^{-1}\mu = 20[deg]$. A sufficient condition for achieving the requirement is equivalent to finding the torque set enabling the total force set f_o' (including the gravitational force) to produce into the hatched area, where the boundaries given by t_1 and t_2 are for always making the object contact with the P-chain and for breaking static frictional condition at the contact point between the object and the P-chain, respectively. To satisfy the sufficient condition, two direction vectors c_{a1} and c_{a2} are prepared as shown in Fig.7(a), where c_{a1} and c_{a2} are chosen so that $c_{ai}^t t_i = 0 (i = 1, 2)$. Giving c_{a1} and c_{a2}, we can obtain the command torque set as shown in Fig.7(b), where $T_c = T_{a1} \cap T_{a2}$. If we choose a set of command torque from T_c, the object is guaranteed to move upward along the P-chain. Fig.8(a) shows an example of 3D model, where we assume two T-chains and one P-chain. The problem is to obtain the torque set enabling the object to move the upper direction, where $l = 1[m], R = 0.2[m], mg = 1.0[N]$, $\tau_i^{min} = 0.0[Nm]$, $\tau_i^{max} = 5.0[Nm]$ (i = 1, 2), and $\alpha = tan^{-1}\mu = 10[deg]$.
In the simulation, we approximate the friction cone by four faced polyhedral cone including the original cone. Fig.8(b) shows the torque set enabling the object to move the designated direction.

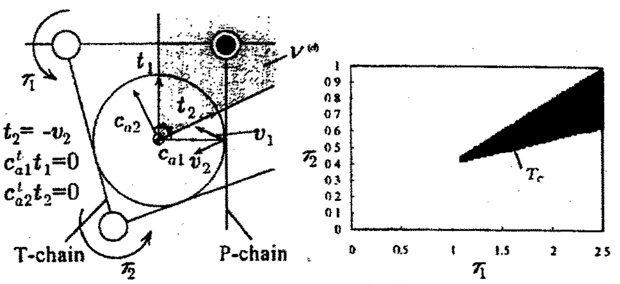

(a) Model (b) Computed torque set

Figure 7: 2D model

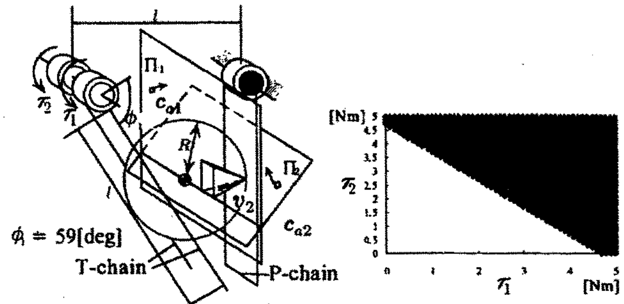

(a) 3D Model (b) Computed torque set

Figure 8: 3D model

4 Experiments

To also confirm the idea, we have done a couple of experiments by utilizing the Hiroshima-hand with the capability of joint level torque control, where the basic mechanical structure is precisely described in [14]. Fig.9 shows a series of experimental results, where the two right fingers are chosen as P-chains and the left one as a T-chain, and the slopes of P-chains are 60[*deg*] and 90[*deg*] in Fig.9 (a) and (b), respectively. It can be seen from these figures that a cylindrical object is lifted up along P-fingers not only by sliding but also by rolling. We have also succeeded in achieving more complicated motions including a switching phase from one direction to another.

5 Concluding Remarks

We have shown a sufficient condition for locally manipulating an object in Envelope Family, by assigning all chains into either T-chain or P-chain. It is important to note that the sufficiency is preserved as far as an approximated friction cone includes the original one. This allows us to approximate each friction cone by a three-faced polyhedral cone which is the polyhedral cone with the minimum number of face. This is an advantageous feature, since it contributes to finding a solution efficiently by reducing the number of inequality set.

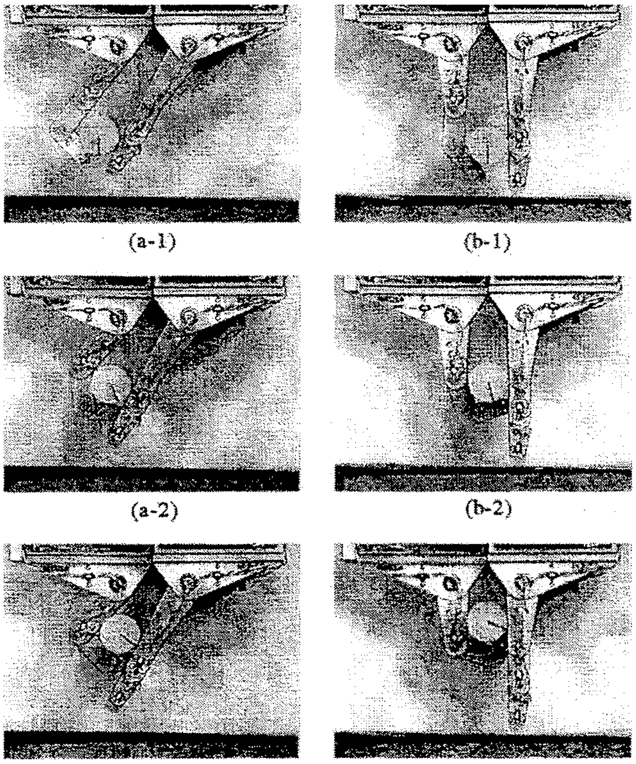

(a) Slope with 60(deg) (b) Slope with 90(deg)

Figure 9: Experimental results

Finally, the authors would like to express their sincere thanks to Mr. Tatsuya Shirai and Mr. Mitsushi Sawada for their simulation and experimental works.

References

[1] Salisbury, J. K., Whole-arm manipulation, *Proc. of the 4th Int. Symp. of Robotics Research*, Santa Cruz, CA, 1987. Published by the MIT Press, Cambridge MA.

[2] Trinkle, J. C., J. M. Abel, and R. P. Paul: Enveloping, frictionless planar grasping, *Proc. of the IEEE Int. Conf. on Robotics and Automation*, 1987.

[3] Mirza, K., and D. E. Orin: Control of force distribution for power grasp in the DIGITS system, *Proc. of the IEEE 29th CDC Conf.*, pp1960-1965, 1990.

[4] Bicchi, A: Force distribution in multiple whole-limb manipulation, *Proc. of the IEEE Int. Conf. on Robotics and Automation*, pp196-201, 1993.

[5] Zhang, X-Y., Y. Nakamura, K. Goda, and K. Yoshimoto: Robustness of power grasp, *Proc. of the IEEE Int. Conf. on Robotics and Automation*, pp2828-2835, 1994.

[6] Zhang, Y., and W. A. Gruver: Definition and force distribution of power grasps, *Proc. of the IEEE Int. Conf. on Robotics and Automation*, pp1373-1378, 1995.

[7] Omata, T., and K. Nagata: Rigid body analysis of the indeterminate grasp force in power grasps, *Proc. of the IEEE Int. Conf. on Robotics and Automation*, pp1787-1794, 1996.

[8] Yu, Y., K. Takeuchi, and T. Yoshikawa: Optimization of robot hand power grasps, *Proc. of the IEEE Int. Conf. on Robotics and Automation*, pp3341-3347, 1998.

[9] Kaneko, M., M. Higashimori, and T. Tsuji: Transition stability of enveloping grasps, *Proc. of the IEEE Int. Conf. on Robotics and Automation*, pp3040-3046, 1998.

[10] Omata, T., and P. DAENGTAMAI: Grasp Force Computing for Power Grasping satisfying External Force Measure, *Proc. of RSJ Annual Conf.*, pp177-178, 1999.

[11] Hirai, S., and H. Asada: "Kinematics and Statics of Manipulation using the Theory of Polyhedral Convex Cones", Int. J. of Robotics Research, vol.12, no.5, pp434-447, 1993.

[12] J.Kerr and B.Roth: "Analysis of multifingered hands ", Int. J. of Robotics Research, vol.4, no.4, pp3-17, 1986.

[13] Rockafellar, R. T.: Convex Analysis, *Princeton University Press*, p16, 1977.

[14] Imamura, N., M. Kaneko, and T. Tsuji: Development of three-fingered robot hand with a new design concept, *Proc. of the 6th IASTED Int. Conf. on Robotics and Manufacturing*, pp44-49, 1998.

Appendix (Proof of Theorem 2)

(1) For example, see [13]. (2) Consider $C' = C_1 + \cdot + C_{n-1}$. From (1), C' is also a polyhedral convex set. Now, consider three vectors $x' \in C'$, $x_n \in C_n$, and $x \in C$ where $x = x' + x_n$. Let P', P_n and P be points expressing the tip of vectors, respectively. Suppose that P and P' denote a vertex in C and a vertex in C', respectively. If P_n exists inside of C_n, we can always make a small sphere whose center is located at P_n as shown in Fig.3. This leads to a contradiction, since $x(=x'+x_n)$ is assumed to be a vertex in C. Therefore, P_n should be a point on the boundary of C_n. Now, suppose that P_n exists on either a plane or an intersection between two planes forming the boundary of C_n. Due to $x = x' + x_n$, P should also be on a plane or a line instead of a vertex, which again lead to a contradiction. Therefore, P_n should be a vertex in C_n. These discussions prove the former part of (2). We can easily find an example of convex set, where a vertex of C_n corresponds to an inner point of C, which supports the correctness of the later part of (2). □